SECURITY CLASSIFICATION OF THIS PAGE

(2)

REPORT DOCUMENTATION PAGE

AD-A215 680

1b. RESTRICTIVE MARKINGS: None

3. DISTRIBUTION/AVAILABILITY OF REPORT: Unlimited

4. PERFORMING ORGANIZATION REPORT NUMBER(S): interim technical report #33

5. MONITORING ORGANIZATION REPORT NUMBER(S):

6a. NAME OF PERFORMING ORGANIZATION: Department of Chemistry

6b. OFFICE SYMBOL (If applicable):

7a. NAME OF MONITORING ORGANIZATION: Office of Naval Research

6c. ADDRESS (City, State, and ZIP Code): Massachusetts Institute of Technology, 77 Mass. Avenue, Bldg. 6-335, Cambridge, MA 02139

7b. ADDRESS (City, State, and ZIP Code): Chemistry Division, 800 N. Quincy Street, Arlington, VA 22217

8a. NAME OF FUNDING/SPONSORING ORGANIZATION: Office of Naval Research

8b. OFFICE SYMBOL (If applicable):

9. PROCUREMENT INSTRUMENT IDENTIFICATION NUMBER: N00014-84-K-0553

8c. ADDRESS (City, State, and ZIP Code): Chemistry division, 800 N. Quincy Street, Arlington, VA 22217

10. SOURCE OF FUNDING NUMBERS

PROGRAM ELEMENT NO.	PROJECT NO.	TASK NO.	WORK UNIT ACCESSION NO.
		051-579	

11. TITLE (Include Security Classification): Direct Measurements of the Physical Diffusion of Redox Active Species....

12. PERSONAL AUTHOR(S): Stuart Licht, Vince Cammarata, and Mark S. Wrighton

13a. TYPE OF REPORT	13b. TIME COVERED	14. DATE OF REPORT (Year, Month, Day)	15. PAGE COUNT
technical interim	FROM 7/1/89 TO 10/1/89	October 1, 1989	55

16. SUPPLEMENTARY NOTATION: prepared for publication in the Journal of Physical Chemistry

17. COSATI CODES		
FIELD	GROUP	SUB-GROUP

18. SUBJECT TERMS (Continue on reverse if necessary and identify by block number): microelectrochemical arrays; diffusion coefficients electrolyte aqueous media

19. ABSTRACT (Continue on reverse if necessary and identify by block number)

See Attached Sheet

20. DISTRIBUTION/AVAILABILITY OF ABSTRACT: ☐ UNCLASSIFIED/UNLIMITED ☐ SAME AS RPT. ☐ DTIC USERS

21. ABSTRACT SECURITY CLASSIFICATION: Unlimited

22a. NAME OF RESPONSIBLE INDIVIDUAL: Mark S. Wrighton

22b. TELEPHONE (Include Area Code): 617-253-1597

22c. OFFICE SYMBOL:

DD FORM 1473, 84 MAR — 83 APR edition may be used until exhausted. All other editions are obsolete.

SECURITY CLASSIFICATION OF THIS PAGE

ABSTRACT

We report methodology for direct measurement of the physical diffusion of molecular species in solution. Movement of a small number of species in solution can be tracked as a function of space and time by using an array of individually addressable microelectrodes. The arrays typically consist of eight, parallel microelectrodes ~50 μm long x ~2.7 μm wide x ~0.1 μm thick separated from each other by ~1.4 μm. Experimental studies and simulations involve electrochemical generation of as few as 6×10^{-20} moles of redox active species at one microelectrode (generator) and electrochemical detection of a significant percentage of these species at other microelectrodes (collection) 0.8 to 26 μm away. The measurements involve the determination of the time dependence of the collector current associated with detection of the diffusing species produced in short and long pulses at the generator. Microelectrochemical experiments and numerical simulations are presented to show that the time dependence of the collector current allows determination of the diffusion coefficient of the diffusing species. For the geometries of generator and collector used an important relationship for short generator pulses is $t_{mt} = 0.22d^2/D$ where t_{mt} is the time associated with the peak in the collector current, d is the distance from the center of the generator to the nearest edge of the collector, and D is the diffusion coefficient. Thus, by knowing d and measuring t_{mt}, D can be determined

for a species generated at one microelectrode and detected at another. Experimental results to demonstrate and verify the methodology relate to studies of the electrochemical generation of $Ru(NH_3)_6^{2+}$, from reduction of $Ru(NH_3)_6^{3+}$, and measurement of its diffusion in aqueous electrolyte having variable amounts of sucrose to adjust D. Einstein-Smoluchowski simulations of the movement of each species of a large set quantitatively predict the diffusion characteristics found experimentally.

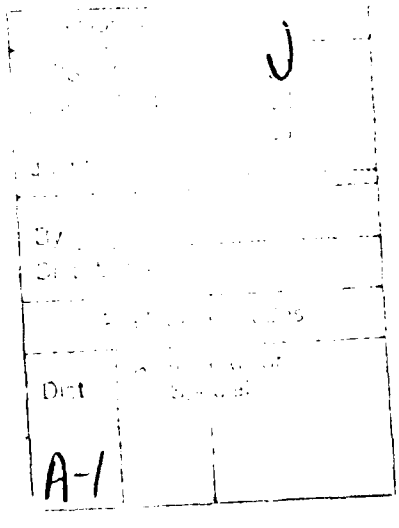

Office of Naval Research

Contract N00014-84-K-0553

Task No. 051-597

Technical Report #33

Direct Measurements of the Physical Diffusion of Redox Active Species: Microelectrochemical Experiments and Their Simulation

by

Stuart Licht, Vince Cammarata, and Mark S. Wrighton

Prepared for Publication

in

Journal of Physical Chemistry

Massachusetts Institute of Technology
Department of Chemistry
Cambridge, MA 02139

DL/1113/89/1

TECHNICAL REPORT DISTRIBUTION LIST, GENERAL

	No. Copies
Office of Naval Research Chemistry Division, Code 1113 800 North Quincy Street Arlington, VA 22217-5000	3
Commanding Officer Naval Weapons Support Center Attn: Dr. Bernard E. Douda Crane, IN 47522-5050	1
Dr. Richard W. Drisko Naval Civil Engineering Laboratory Code L52 Port Hueneme, California 93043	1
Defense Technical Information Center Building 5, Cameron Station Alexandria, Virginia 22314	2 high quality
David Taylor Research Center Dr. Eugene C. Fischer Annapolis, MD 21402-5067	1
Dr. James S. Murday Chemistry Division, Code 6100 Naval Research Laboratory Washington, D.C. 20375-5000	1
Dr. Ronald L. Atkins Chemistry Division (Code 385) Naval Weapons Center China Lake, CA 93555-6001	1
Chief of Naval Research Special Assistant for Marine Corps Matters Code 00MC 800 North Quincy Street Arlington, VA 22217-5000	1
Dr. Bernadette Eichinger Naval Ship Systems Engineering Station Code 053 Philadelphia Naval Base Philadelphia, PA 19112	1
Dr. Sachio Yamamoto Naval Ocean Systems Center Code 52 San Diego, CA 92152-5000	1
David Taylor Research Center Dr. Harold H. Singerman Annapolis, MD 21402-5067 ATTN: Code 283	1

[Prepared for publication in the *Journal of Physical Chemistry*]

Direct Measurements of the Physical Diffusion of Redox Active Species: Microelectrochemical Experiments and Their Simulation

Stuart Licht,[1] Vince Cammarata, and Mark S. Wrighton*

Department of Chemistry

Massachusetts Institute of Technology

Cambridge, Massachusetts 02139

*Address correspondence to this author.

ABSTRACT

We report methodology for direct measurement of the physical diffusion of molecular species in solution. Movement of a small number of species in solution can be tracked as a function of space and time by using an array of individually addressable microelectrodes. The arrays typically consist of eight, parallel microelectrodes ~50 μm long x ~2.7 μm wide x ~0.1 μm thick separated from each other by ~1.4 μm. Experimental studies and simulations involve electrochemical generation of as few as 6×10^{-20} moles of redox active species at one microelectrode (generator) and electrochemical detection of a significant percentage of these species at other microelectrodes (collection) 0.8 to 26 μm away. The measurements involve the determination of the time dependence of the collector current associated with detection of the diffusing species produced in short and long pulses at the generator. Microelectrochemical experiments and numerical simulations are presented to show that the time dependence of the collector current allows determination of the diffusion coefficient of the diffusing species. For the geometries of generator and collector used an important relationship for short generator pulses is $t_{mt} = 0.22d^2/D$ where t_{mt} is the time associated with the peak in the collector current, d is the distance from the center of the generator to the nearest edge of the collector, and D is the diffusion coefficient. Thus, by knowing d and measuring t_{mt}, D can be determined

for a species generated at one microelectrode and detected at another. Experimental results to demonstrate and verify the methodology relate to studies of the electrochemical generation of $Ru(NH_3)_6^{2+}$, from reduction of $Ru(NH_3)_6^{3+}$, and measurement of its diffusion in aqueous electrolyte having variable amounts of sucrose to adjust D. Einstein-Smoluchowski simulations of the movement of each species of a large set quantitatively predict the diffusion characteristics found experimentally.

We wish to report the use of microelectrode arrays to measure diffusion coefficients in electrolyte media. The utility of microelectrode arrays stem from the small size of the microelectrodes, their close spacing, and the reproducible geometry produced by microlithography. The precise measurement of diffusion coefficients and the elucidation of diffusional processes are necessary for better understanding of phenomena in a number of disciplines. In electrochemistry the diffusion coefficient of redox molecules ultimately determines the transport rate of substrate to the electrode surface.[2] The diffusion coefficient can be used to determine hydrodynamic radii (Stokes radii) of dissolved species reflecting their solvation number.[3] Measurements of diffusion coefficients can be used to understand the behavior of solutes in viscous polymer-containing solutions.[4]

Recently, the spatial resolution of the diffusion layer near an electrode has been the subject of a number of investigations. Microelectrodes have been used to map this layer within 5 μm of a macroscopic electrode.[5] Light beams have been employed to elucidate the concentration profiles within the diffuse layer.[6] Internal reflectance spectroscopy has been used to obtain IR and UV-Vis spectra of species formed close to the electrode surface.[7] These techniques have helped to elucidate the steady-state concentration profiles of the diffusion layer.

In 1984, our research group introduced closely-spaced arrays of eight microelectrodes, fabricated using microlithographic techniques.[8] The introduction of closely-spaced microelectrode arrays provides a very small gap over which one can observe the diffusion of species.[9] Microelectrode arrays have been covered with electronic and redox conducting polymers to measure intrinsic properties such as conductivity and diffusion coefficients for charge transport.[10,11] The experiments in this work are referred to as generation-collection experiments. One microelectrode, termed the "generator", produces a species electrochemically which diffuses outward, away from the generator. Nearby microelectrodes termed "collectors" indicate the local concentration of the diffusing species also electrochemically. In steady-state generation-collection experiments the generator produces a diffusion-limited flux of species, and the collector detects that species by reversing the electrochemical step. Steady-state generation-collection experiments can exhibit large collection efficiencies,[12] where collection efficiency is defined as the ratio of the collector to the generator currents.

Although steady-state generation-collection experiments allow determination of absolute collection efficiencies, such experiments do not allow direct measurements of the physical diffusion of species produced at the generator. Murray and coworkers introduced "time of flight"

microelectrochemical experiments to measure the diffusion of carriers in redox polymers.[11] The method involves pulsed generation of the diffusing species and steady-state detection. We have extended the method introduced for studying charge transport to study physical diffusion in electrolyte media. Scheme I presents a representation of the methodology for measurements of the diffusion of an electrochemically generated reduced species 'red'. An electrolyte solution is prepared containing only 'ox', the oxidized form of 'red'. Initially, the generator and collector electrodes are maintained at a potential, E_{ox}, positive of $E^{o'}$(ox/red). The generator is then stepped or pulsed to a reducing potential, E_{red}, negative of $E^{o'}$(ox red), producing 'red' which is monitored as cathodic current, I_{Gen}. As 'red' diffuses away from the generator, the time variation of the collector current, I_{Col}, indicates arrival, collection, and re-oxidation to 'ox'. For a fixed geometry of generator and collector, the diffusion coefficient, D, of the electrogenerated species governs the time dependence of I_{Col}. Scheme II shows a representation of the generator potentials and collector responses for both the pulsed and stepped potential experiments. Similarly, diffusion characteristics of an oxidized species may be studied through application of an oxidizing potential in an electrolyte which initially only contains the reduced form of the species to be studied.

As will be shown, our method for studying diffusion by generation-collection experiments is analogous to studying transients at rotating ring-disk electrodes[13] with a few important exceptions. First, no rotational perturbations to the system are required. Second, the microelectrode array can have many collector electrodes as opposed to only one ring electrode and the distance between the generator and collector electrodes may be easily varied. Third, collection efficiencies can be much higher. Finally, the transit time for movement from the generator to the collector can be more than an order of magnitude shorter than for thin-gap rotating ring-disk electrodes.[13]

In this article we wish to report our methodology for measurement of diffusion using microelectrode arrays. In a preliminary note we extended the concept introduced by Murray[11] and showed its application to monitoring very small quantities of redox-active ions in solution.[9] The utility of this technique for measuring physical diffusion in a solid polymer electrolyte has been demonstrated in the diffusion coefficient determination of Ag^+.[14] Presented here is a full account of our experimental and simulation procedures for studying physical diffusion using microelectrode arrays.

EXPERIMENTAL SECTION

Microelectrode Arrays. Two types of microelectrode arrays were used in this work. "Longer arrays" of eight Au microelectrodes had dimensions of ~70 μm long, 2.74 μm wide, and 0.1 μm thick and spaced 1.37 μm apart. Fabrication of the microelectrode arrays on p-Si/SiO_2/Si_3N_4 subtrates has been described previously.[8,15] "Shorter arrays" consisted of six microelectrodes of dimensions 6 μm long, 1.3 μm wide and 0.1 μm thick and spaced 0.8 μm apart. The fabrication of these microelectrode arrays involves procedures similar to those used for the longer arrays and will be described in detail elsewhere.[16] Microelectrode dimensions were determined using a Cambridge Mark 2A Stereoscan electron microscope and a Bausch & Lomb MicroZoom microscope. The device surface, except for the electrochemically active area was encapsulated using Hysol Corporation clear and white epoxies.

Prior to use, arrays, mounted on electrically accessible transistor headers, were sonicated for several minutes in acetone to remove residual photoresist. This was followed by a chemical etch for 10 s in a fresh 3:1 solution of concentrated H_2SO_4 and 30% H_2O_2 and then rinsed with Omnisolv H_2O. The etch/rinse was repeated twice with only a 3 s etch. Substantially longer etches reduced observed electrode dimensions.

Clean, dry microelectrode arrays were tested for electrical isolation of each microelectrode of the array.

Microelectrodes with an intermicroelectrode resistance of greater than 10^8 were considered to be isolated. Arrays were then immersed in an aqueous 0.1 **M** K_2HPO_4 solution for an electrochemical cleaning by potentiostatic cycling of each electrode between -1.5 and -2.0 V vs. saturated calomel electrode (SCE) at 100 mV/s for 10 s, to evolve H_2. A final characterization for electrode isolation and electrochemical activity of the array was carried out in a 5 m**M** solution of $Ru(NH_3)_6Cl_3$ in 0.1 **M** KCl. Individual and adjacent pairs of microelectrodes were cycled between 0.3 and -0.6 V vs. SCE. Such a test reveals, for a single "active" microelectrode, a sigmoidal current-voltage curve with a plateau current of 20-25 nA for the longer arrays and ~6 nA for the shorter arrays.

Chemicals. Electronic grade solvents were used for chemical etching. Omnisolv H_2O was used as a solvent for all electrolytes. All other chemicals were analytical grade and were used as received, with the exception of $Ru(NH_3)_6(ClO_4)_3$ which was prepared by precipitation of $Ru(NH_3)_6Cl_3$ (Alfa) from aqueous $NaClO_4$ solutions. In electrochemical studies conducted on the order of days, Au microelectrode array electrodes proved to be more durable in aqueous $NaClO_4$ rather than KCl environments. After ~1 day in 0.1 **M** KCl, chemical attack of the Au arrays was evident, although the observed $Ru(NH_3)_6(ClO_4)_3$ solubility (~2.5 m**M** in 0.1 **M** $NaClO_4$) is substantially less than that for $Ru(NH_3)_6Cl_3$. Sucrose was obtained from Mallinckrodt. Viscosity

measurements as reported[9] were also verified by Ostwald measurements in a long capillary tube.

Equipment. Cyclic voltammetry measurements were carried out using a 100 nA scale modified Pine Instruments RDE-4 bipotentiostat and a Kipp and Zonen BD 91 X-Y-Y' recorder. Two experimental setups were used to record microelectrode transit times measurements. In the less sensitive experiments both working electrodes of the RDE-4 were employed, one to generate and record potential pulse excursions and the second to fix the collector potential and record the current. In the most sensitive experiments the potential step and potential pulse signals were applied using a two-electrode configuration with a Princeton Applied Research 175 Universal Programmer. The collector was held at various potentials in a three-electrode configuration with a Bioanalytical Systems BAS100 Low Current Module and the signals stored on a Nicolet 4904 Digital Collection Oscilloscope. Digital Simulations were performed on a 640K IBM PC XT with Intel 8087 Math Coprocessor, using Microsoft Fortran modified to incorporate DOS ANSI.SYS. The source code for the digital simulations is included as supplementary material.

RESULTS AND DISCUSSION

Generation-Collection Cyclic Voltammetry of $Ru(NH_3)_6^{2+/3+}$. Cyclic voltammetry at closely spaced microelectrodes has previously been studied and generation-collection experiments have been simulated.[12] In our new work the simulation used gives somewhat better agreement with experiment. In generation-collection experiments species generated at one microelectrode may be collected at nearby parallel microelectrodes. Collection efficiency, Φ_{ss}, is the ratio of the steady-state collector current to the steady-state generator current in the cyclic voltammograms. We present typical experimental results from cyclic voltammetry in Figure 1. As shown in Figure 1, a large fraction of electrogenerated $Ru(NH_3)_6^{2+}$ may be collected. The fraction depends on the number and geometry of the collector electrodes. In Figure 1 $Ru(NH_3)_6^{2+}$ was produced by reduction of $Ru(NH_3)_6^{3+}$ at a 2.74 μm wide generator electrode and was collected at collector electrodes with edges spaced from 1.37 to 26.03 μm from one edge of the generator (center to edge distances ranging from 2.74 to 27.4 μm). Φ_{ss}'s ranged from 58% to 68% with simultaneous utilization of electrodes 2 to 2-7 respectively as collector electrodes using 1 as the generator electrode (with reference to Scheme I). The observed values of Φ_{ss} are reproducible to ±1% on a variety of arrays tested. Note in Figure 1 that the generator current is enhanced by the regeneration of $Ru(NH_3)_6^{3+}$ at the collector. This

"feedback" effect has been discussed and modeled earlier,[12] and is a consequence of the close electrode spacings.

As previously reported,[12] Φ_{ss} increases from 19% to 58% for a single collector as the separation from generator to collector is decreased from 26.03 to 1.37 μm. Utilization of two collector electrodes, located on each side of a central generator, results in collection efficiencies which increase from 56% to 83% as the separation between generator and each of the collectors is decreased from 9.59 to 1.37 μm. Utilization of 2 to 6 collector electrodes, half of which are located on either side of a center generator, results in Φ_{ss}'s which increase from 83% for 2 collectors to 88% for 6 collectors.

Ru(NH$_3$)$_6^{2+}$ Diffusivity. The diffusion coefficient of Ru(NH$_3$)$_6^{2+}$ has not been previously reported. In order to independently verify diffusion coefficients from microelectrode measurements, the Ru(NH$_3$)$_6^{2+}$ diffusion coefficient was measured by determining the limiting current in microdisk cyclic voltammetry.[17] Figure 2 presents representative comparative microelectrode cyclic voltammetry for the same microdisk electrode in 5.0 mM solutions of Fe(CN)$_6^{4-}$, Ru(NH$_3$)$_6^{3+}$ and Ru(NH$_3$)$_6^{2+}$. In the identical electrolytic medium utilized, the limiting steady-state redox currents reflect the relative diffusivity of the three species. The inset is a plot of limiting current vs. concentration. From the relative slopes of the plots of current vs. concentration D can be determined for Ru(NH$_3$)$_6^{2+}$

by knowing D for $Fe(CN)_6^{4-}$ or $Ru(NH_3)_6^{3+}$. From the known diffusion coefficients for $Ru(NH_3)_6^{3+}$ and $Fe(CN)_6^{4-}$ of 7.1 x 10^{-6} cm^2/s,[12] and 6.5 x 10^{-6} cm^2/s,[18] respectively, the diffusion coefficient of $Ru(NH_3)_6^{2+}$ is determined as 7.8 $\pm$ 0.1 x 10^{-6} cm^2/s at 20°C in 0.1 **M** KCl. The value of D for $Ru(NH_3)_6^{2+}$ in 0.1 **M** $NaClO_4$ is found to be the same, within experimental error, as in 0.1 **M** KCl.

Pulsed Transit Time Measurements. Application of a short electrochemical generation pulse allows measurement of the time for transit of the generated species to a collector. Square wave potential pulses of various duration were applied to a generator electrode to produce a "pulse" of $Ru(NH_3)_6^{2+}$ via reduction of $Ru(NH_3)_6^{3+}$. The resulting I_{col} was monitored as a function of time. Generation and movement of $Ru(NH_3)_6^{2+}$, reductively formed at a generator electrode, was studied in approximately millimolar concentration solutions of $Ru(NH_3)_6^{3+}$. The results of typical microelectrode transit time determinations are presented in Figure 3 for pulsed generation-collection measurements utilizing adjacent microelectrodes. In this figure, the I_{col} at a microelectrode is shown as a function of time following generation pulses varying from 2 to 50 µs. Significantly, the position of I_{col}(peak) and shape of the plot of I_{col} vs. time is independent of the duration of the generator pulse for the pulse durations used. For the 2 µs pulse the collector current reflects the distribution in time of the resultant 1.6 x 10^{-14} C, and arrival of

7×10^{-20} moles, or 40,000 species. As seen in the figure inset, the number of species arriving at the collector varies linearly with pulse durations over the range from 2 μs through 2 ms.

As seen in Figure 3, subpicoampere currents, following a generator potential pulse as short as 2 μs, are detectable at the collector microelectrode in less than 10^{-3} seconds, with best results resolvable to detection of the arrival of an equivalent of 10^{-16} C of the produced species (less than 1000 discrete species). The integration of the shortest pulses is presented in our preliminary account of this work.[9] Minimum detectable pulses are limited by faradaic shielding, numerical conditioning techniques, and the available time and current resolution of the BAS100 Low Current Module used.

In the pulsed microelectrode transit time experiment, as typified by data in Figure 3, a key measurement is t_{mt}, the time of maximum collection rate, I_{col}(peak), Scheme II. With reference to t_{mt} it is possible to define what is meant by short and long generation pulses. In short pulse experiments the pulse duration used is < 1/3 t_{mt}. For a 1.37 μm generator-collector separation I_{col}(peak) occurs at t_{mt} = 2.9 ($\pm$0.1) ms. Experiments with generator and collector electrodes separated by 26 μm gave I_{col}(peak) at t_{mt} = 215 ms to within a reproducibility of 3%.

Microelectrode Transit Time Variation with Distance. Figure 4 summarizes pulsed microelectrode transit time measurements

for $Ru(NH_3)_6^{2+}$ produced at a generator microelectrode as monitored at each of seven nearby collector microelectrodes. The figure inset shows an inverse square relationship between t_{mt} and the generator to collector distance as described by equation (1). Only in the case of adjacent

$$t_{mt} \alpha d^2 \qquad (1)$$

generator and collector microelectrodes is the electrode width of 2.74 μm substantial compared to the interelectrode separation of 1.37 μm. The distance, d, as measured from the center of the generator electrode to the collector electrode edge gives the best linear plot of t_{mt} vs. d^2 having a zero intercept. The d^2 dependence of t_{mt} is expected for a diffusion governed movement of the electrogenerated species from generator to collector.

Diffusion Coefficient Dependence of Transit Times. Figure 5 shows microelectrode transit time measurements for $Ru(NH_3)_6^{2+}$ produced at a generator microelectrode and as monitored at a collector microelectrode 6.85 μm from the generator. Experiments were conducted in 2.5 m**M** $Ru(NH_3)_6(ClO_4)_3$, 0.1 **M** aqueous $NaClO_4$ containing various concentrations of sucrose to vary the value of D. Actual values of D were determined as described above for KCl solutions and illustrated in Figure 2. The generator electrode was pulsed from 0.0 to -0.4 V vs. SCE while the

collector electrode was maintained at 0.0 V vs. SCE. Solutions contained 0 to 48% sucrose by weight with viscosities ranging from η = 1.00 to 12.5 cP. In aqueous solutions containing up to 48% sucrose, D has been shown to vary inversely with viscosity.[19] The inset of Figure 5 shows that t_{mt} is inversely proportional to D, equation (2). Thus, the distance dependence of t_{mt}, equation (1), and

$$t_{mt} \alpha 1/D \tag{2}$$

the diffusion coefficient dependence of t_{mt}, equation (2), yield the result shown in equation (3). The constant of

$$t_{mt} = 0.22d^2/D \tag{3}$$

proportionality, 0.22 $\pm$ 0.02, is empirically determined by measuring t_{mt} where d and D are known.

Stepped Microelectrode Transit Time Measurement. The results of typical potential step (long pulse, >> t_{mt} from short pulse experiments) microelectrode experiments are presented in Figure 6. Potential steps were applied to a generator electrode and the resulting I_{col} monitored as a function of time, Scheme II. As seen in Figure 6, the time variation of I_{col}, induced by potential step generated currents of approximately 10^{-8} A, depends on the collector-generator separation, and typically requires several seconds

to reach nearly steady-state currents for the separations shown.

For the stepped generator experiment, the time dependence of the I_{col} is similar to the time dependence of the integrated I_{col} in pulsed potential microelectrode transit time experiments.[9] The relevant dynamic parameter in the stepped generator experiments is the time to achieve a given percentage of the steady-state collection current. In the case in which the generator-collector separation is 1.37 μm, the collector current achieves one-third and two-thirds of the steady-state collector current at 4.0 (±0.3) and 18 (±0.9) ms, respectively.

Stepped generator microelectrode transit times were measured between generator and collector microelectrodes separated by a gap of as small as 0.8 μm. In this case, a microelectrode transit time of approximately 0.5 ms is observed for $Ru(NH_3)_6^{2+}$ to achieve 2% of the steady-state collection current. This can be compared to rotating ring-disk electrodes where for a thin gap (r_2/r_1 = 1.07), at 1000 rpm, 2% of steady-state values occur in 30 ms,[20] and reflects the capability of microelectrode transit time experiments to access considerably faster time regimes than conventional rotating ring-disk experiments.

Stepped Transit Times as a Function of Distance and Diffusion Coefficient. Using data from the step microelectrode transit time measurements exemplified in Figure 6, $t_{1/3}$ and $t_{2/3}$ (defined as the time to reach 1/3

and 2/3 of the steady-state collection currents, respectively) can be determined as a function of distance, d. These times are presented in Figure 7 for $Ru(NH_3)_6^{2+}$ generated and collected at a variety of distances from the generation source. The figure shows that $t_{1/3}$ and $t_{2/3}$ are proportional to d^2, as expected for a diffusion process.

Figure 8 summarizes step microelectrode transit time measurements as a function of diffusion coefficient, D, for $Ru(NH_3)_6^{2+}$ produced at a generator microelectrode and as monitored at a collector microelectrode 6.85 μm from the generator. Variation in D was achieved by using different sucrose concentrations. The step microelectrode transit times $t_{1/3}$ and $t_{2/3}$ exhibit a linear increase with viscosity, η, and 1/D. Thus, the data in Figures 7 and 8 show $t_{1/3}$ and $t_{2/3}$ to be proportional to d^2/D. The data can be summarized by equations (4) and equation (5), where the constants of proportionality are determined by measurements

$$t_{1/3}\ (\text{experimental}) = 0.37d^2/D \qquad (4)$$

$$t_{2/3}\ (\text{experimental}) = 1.34d^2/D \qquad (5)$$

of $t_{1/3}$ and $t_{2/3}$ where d and D are known.

Microelectrode Transit Time Random Walk Simulation. Simulations of diffusion have traditionally used Fick's Law, equation (6), to model concentration flux. Such models have

$$\partial C/\partial T = -D(\partial^2 C/\partial X^2 + \partial^2 C/\partial Y^2) \quad \text{(for two dimensions)} \quad (6)$$

been applied to linear, cylindrical, and spherical geometry systems,[21] and generally involve numerical integration of spatial elements in all but the simplest one-dimensional cases. A fundamentally equivalent, but simpler starting point involves use of the Einstein-Smoluchowski equation[22,23] describing the unit time element, τ, for random movement ΔX or ΔY in a system as in equation (7).

$$\tau_X = (\Delta X)^2/4D \qquad \text{(for two dimensions)} \qquad (7)$$

The development of a model which assumes the random behavior of individual species of an ensemble, rather than the statistical properties of an ensemble, is attractive as our experiments begin to approach the realm of discrete particle behavior. The experiments presented here involve the behavior of less than 10^5 species in the smallest ensemble, but the data are resolvable to ~1000 species with existing procedures. As a model for our current experiments, a digital simulation of the individual random movements of 10^5 particles was done which is computationally viable with modern microcomputers.

To better understand factors governing generation-collection efficiencies and to visualize the microelectrode transit time experiments we have carried out numerical simulations. Figure 9 presents the geometry used for a two-

dimensional Einstein-Smoluchowski based random walk simulation of transit time and collection efficiencies in generator-collector microelectrode experiments. A cross sectional plane of the parallel microelectrodes is depicted in which a pulse of individual redox units (to simulate pulsed microelectrode transit time) or a constant addition of individual redox units (to simulate stepped microelectrode transit time experiments) are introduced into the model at the indicated generator sites. Each concentration unit, characterized by diffusion coefficient, D, will randomly move a distance, ΔX or ΔY (set equal to an experimentally utilized interelectrode gap of 1.37 μm), during each iterative time cycle of duration τ, equation (7). Concentration units arriving at collector sites, C, are counted and removed from solution to indicate electron transfer and collection as a function of time. The collection efficiency is taken to be the number of species collected compared to the number injected into the model space. Numerically simulated collection efficiencies show a random variation of less than 1% when 10,000 or more species are injected into the system. In our simulation we compute over a simulation space of $\pm$55 μm (equivalent to $\pm$40 incremental units ΔX).

Figure 10 shows the concentration profiles of released redox units in a simulation of the microelectrode transit time pulse experiment at various simulation times and for three different collection scenarios: (1) no collection, (2)

collection at one microelectrode and (3) collection at two microelectrodes symmetrically disposed about the generator. These concentration profiles of various collector orientations describe the simulated movement of 10^5 redox units through the simulated geometric space as given in Figure 9. The comparisons from one time to another show the depletion of the injected redox units due to collection. The simulated diffusion coefficient of 7.8×10^{-6} cm^2/s (that of $Ru(NH_3)_6^{2+}$) was chosen so that the greatest concentration of redox units passes the nearest electrodes at about 3 ms. The shading of each box in the simulation space represents the fraction of redox units of the original 10^5 within that box with the darker grays representing larger fractions.

The left set of simulations in Figure 10 show the release of 10^5 redox units at the generator electrode with no collection. At 10 ms the redox units have spread almost entirely across the array of electrodes and show a symmetrical distribution about the central generator. At 100 and 500 ms the concentration profile has expanded considerably and the concentration nearest the generator becomes less, i.e. more dilute. Collection by an electrode three electrodes away from the generator is shown in the center set of simulations. At 10 ms the concentration profile is very similar to the generation only case. At 100 and 500 ms the concentration profiles are more dilute especially near the collector. The 10 ms profile is similar

to that of the no collector case because the maximum of the collection flux occurs at ~41 ms so that depletion of the concentration profile is insignificant at 10 ms. Only at 100 and 500 ms does the concentration profile reflect substantial asymmetric collection of redox units. On the right side of Figure 10 is shown the concentration profiles of symmetric collection with two collectors each three electrodes away from the generator. These profiles can be compared with the center set, the case of only one collector. The latter profiles show fewer redox units left after 500 ms, consistent with greater collection. The symmetry of the concentration profile is maintained throughout the time regimes studied.

Figures 11 and 12 present comparisons of experimental and simulated collection efficiencies, Φ_{SS}, at various distances, from center to edge, between generator and collector microelectrodes and for different collector widths. Experimental collection efficiencies are determined for $Ru(NH_3)_6^{2+}$ in aqueous solutions of $Ru(NH_3)_6^{3+}$ as the ratio of collector to generator currents presented in Figure 1. Diamond, square and open triangles refer respectively to experimental, theoretical (this work), and theoretical using a Fick's law starting point (from reference 12) collection efficiencies for an asymmetric collector electrode located on a single side of the generator electrode. '+', 'X' and solid triangles refer similarly to experimental, theoretical (this work) and theoretical (from reference 12) collection

efficiencies for a pair of collector electrodes situated symmetrically about a central generator. Collector width, in both the experiment and simulation, Figure 12, was increased by utilization of additional parallel 2.74 μm electrodes (collectors) spaced 1.37 μm apart. Experimental collection efficiencies are determined for $Ru(NH_3)_6^{2+}$ in aqueous solutions of $Ru(NH_3)_6^{3+}$ as the ratio of collector to generator currents presented in Figure 1. Diamond and squares refer respectively to experimental and theoretical (this work) collection efficiencies for utilization of from 1 to 7 nearest collector electrodes located on a single side of the generator electrode. '+', 'X' and solid triangles refer respectively to experimental, theoretical (this work) and theoretical (from reference 12) collection efficiencies for 2, 4, 6 or 7 nearest collector electrodes situated about a central generator. Total collector width is given by 2.74 μm multiplied by n, where n is the number of collector microelectrodes utilized.

In Figures 11 and 12 it is seen that our simulation provides an excellent description of steady-state collection efficiencies for all geometries tested. Note also from Figure 9, the relative ease with which a variety of geometrical configurations can be incorporated into the simulation.

Comparison of Simulated and Measured Microelectrode Transit Time. Another test of the simulation procedure is the prediction of dynamic rather than steady-state diffusion.

In Figure 13 simulated and measured transit times, t_{mt}, are compared for $Ru(NH_3)_6^{2+}$, with a diffusion coefficient of 7.8 x 10^{-6} cm^2/s, between 2.74 μm wide generator and collector electrodes, separated by 27.4 μm. As seen on the right hand figure, the variation of the amount collected in time is well predicted by the model. The collector current is in excellent agreement with the simulated temporal behavior for the number of species arriving at the collector. Generally, over the range of generator-collector separations, the simulation predicts microelectrode transit times to be approximately 10% faster than experimentally observed transit times, t_{mt}, equation (8). The empirical constant of

$$t_{mt} \text{ (simulation)} = 0.20d^2/D \qquad (8)$$

proportionality, 0.22, in equation (3) has an experimental uncertainty of approximately 10%, however. Thus, the simulation of both steady-state and dynamic generation-collection experiments is a good way to provide visualization of actual experiments that have been executed.

CONCLUSIONS

Experiments and numerical simulations have been used to show that the time rate of change of fixed array microelectrode generator and collector currents in potential step and pulse measurements can provide a direct determination of diffusion coefficient. Microelectrode transit time measurements have been used for the direct determination of the characteristic space and time behavior of as few as 40,000 redox active species in solution to a resolution of <1000 species. The generation and movement of $Ru(NH_3)_6^{2+}$ from a microelectrode was observed by oxidative collection at independent microelectrodes situated 0.8 to 26 μm from the generation source. Einstein-Smoluchowski simulations have been used to quantitatively predict each experimental characteristic. Our technique extends the time of flight methodology introduced earlier,[11] and has been used to monitor Ag^+ diffusion in a solid polymer electrolyte where rotating electrode techniques are not applicable.[14] Additionally we have used this technique to determine the diffusion characteristics of reduced and oxidized cytochrome c which will be the focus of a subsequent paper.[24]

The constants of proportionality in equations (3), (4), and (5) hold for our 6 μm and 70 μm long microelectrode arrays. The constant of proportionality in the simulation also is within the error limits of the experimental measurements. The important point from both the experiments and the simulation is that (3)-(5) hold for a geometry of

generator and collector which are long and parallel to one another. It is interesting that the constants of proportionality are essentially fixed in the case of the 6 μm long microelectrodes, considering that d is up to ~26 μm for the largest interelectrode distance. Thus, by measuring t_{max}, $t_{1/2}$ or $t_{2/3}$ it is possible to establish D by knowing d.

The techniques used and results found for $Ru(NH_3)_6^{2+}$ are similar to those of the time of flight measurements used to measure carrier diffusion in redox polymers coating a microelectrode array.[11] Charge transport, in our case, occurs through physical diffusion rather than electron self-exchange for $Ru(NH_3)_6^{2+}$ at the concentrations used in our study.[25] Electron self-exchange is the mechanism for carrier transport in redox polymers, but for the solution redox species the self-exchange process is much slower than physical diffusion owing to the modest self-exchange rate constant, ~10^3 $M^{-1}s^{-1}$,[25] and the low (~5 mM) concentrations used. Our findings therefore do show that transient microelectrochemical techniques can be used to study physical diffusion of solution species, but use of low concentrations is important to insure that the values of D are the true physical diffusion coefficients.

ACKNOWLEDGEMENTS.

We would like to acknowledge Lockheed Missile and Space Company, Inc. and the Office of Naval Research and the

Defense Advanced Research Projects Agency for partial financial support of this research.

SUPPLEMENTARY MATERIAL AVAILABLE:

The random walk simulation is presented here. The source code was written in the ®Microsoft version of Fortran 77 for the IBM PC (12 pages). Ordering information is given on any current masthead page.

REFERENCES

1. Current Address: Department of Chemistry, Clark University, Worcester, MA 01610.

2. Nernst, W. *Z. Physik. Chem.* **1904, 47,** 52.

3. Bockris, J. O'M. *Quart. Rev.* **1949, 3,** 173.

4. Yam, K. L.; Anderson, D. K. ; Buxbaum, R. E. *Science* **1988, 241,** 330.

5. Engstrom, R. C.; Weber, M.; Wunder, D. J.; Burgess, R.; Winquist, S. *Anal. Chem.* **1986, 58,** 844; Engstrom, R. C.; Meaney, T.; Tople, R.; Wightman, R. M. *Anal. Chem.* **1987, 59,** 2005.

6. Rossi, P.; McCurdy, C. W.; McCreery, R. L. *J. Am. Chem. Soc.* **1981, 103,** 2524; Jan, C.-C.; McCreery, R. L. *Anal. Chem.* **1986, 58,** 2771.

7. Winograd, N.; Kuwana, T. *J. Amer. Chem. Soc.* **1971, 93,** 4343.

8. Kittlesen, G.; Wrighton, M. S. *J. Am. Chem. Soc.* **1984, 106,** 5375.

9. Licht, S.; Cammarata, V.; Wrighton, M. S. *Science,* **1989, 243,** 1176.

10. Wrighton, M. S.; Thackeray, J. W.; Natan, M. J.; Smith, D. K.; Lane, G. A.; Belanger, D. *Phil. Trans. Roy. Soc. Lond.* **1987, B 316,** 13.

11. Feldman, B. J.; Feldberg, S. W.; Murray, R. *J. Phys. Chem.* **1987, 91,** 6558.

12. Bard, A. J.; Crayston, J. A.; Kittlesen, G. P.; Shea, T. V.; Wrighton, M. S. *Anal. Chem.* **1986, 58**, 2321.

13. Albery, W. J.; Hitchman, M. L. *Ring-Disc Electrodes;* Oxford University Press: London, **1971.**

14. Cammarata, V.; Talham, D. R.; Crooks, R. M.; Wrighton, M. S. submitted to *J. Phys. Chem.*

15. Wrighton, M. S.; Chao, S.; Chyan, O. M.; Jones, E. T. T.; Leventis, N.; Lofton, E. A.; Schloh, M. O.; Shu, C. F. *Chemically Modified Microelectrode Surfaces in Science and Industry;* Leyden, D. E.; Collins, W. T., Eds.; Gordon and Breach: New York, **1987;** p. 337.

16. Ofer, D. Ph.D. Thesis, Massachussetts Institute of Technology.

17. Kovach, P. M.; Caudill, W. L.; Peters, D. G.; Wightman, R. M. *J. Electroanal. Chem.* **1985, 185**, 285.

18. von Stackelberg, M.; Pilgram, M.; Toome, W. *Z. Elektrochem.* **1953, 57**, 342.

19. Prater, K. B.; Bard, A. J. *J. Electrochem. Soc.* **1970, 117**, 207.

20. Zhang, X.; Yang, H.; Bard, A. J. *J. Am. Chem. Soc.* **1987, 109**, 1916.

21. Urban, P.; Speiser, B. *J. Electroanal. Chem.* **1988, 241**, 17.

22. von Smoluchowski, M. *Ann. Phys. (Paris)* **1908, 25**, 205.

23. Einstein, A. *Investigations on the theory of Brownian movement;* Methuen: London, 1926.

24. Cammarata, V.; Licht, S.; Wrighton, M. S. manuscript in preparation.

25. Meyer, T. J.; Taube, H. *Inorg. Chem.* **1968**, **7**, 2369.

SCHEME AND FIGURE CAPTIONS

Scheme I. Schematic representation of a microelectrode transit time measurement of reduced species. Initially, the generator and collector electrodes are maintained at an oxidizing potential. The generator is pulsed or stepped to a relatively reducing potential, producing the reduced species monitored as a cathodic current through the generator. As the reduced species diffuse away from the generator, the time variation of anodic current at the collector electrode signals arrival, collection, and oxidation of the species. In addition to the indicated dimensions, experiments were also performed on arrays of six 1.3 μm microelectrodes, 6 μm long, each separated by a gap of 0.8 μm.

Scheme II. Schematic representation of the time dependence of generator potential and collector current during a microelectrode transit time measurement. (Upper curves) With reference to Scheme I, the generator is pulsed to a relatively reducing potential. Arrival of the diffusing species at the collector is detected by anodic current. As indicated, t_{mt} is measured as the time from the midpoint of the generator pulse to the point of maximum collector current. (Lower curves) As above, but the generator is stepped to a constant potential and the resultant time dependence of the collector current monitored. As indicated

$t_{1/3}$ or $t_{2/3}$ are measured from the origin of the generator step to the time to acheive 1/3 or 2/3 of the psuedo-steady-state collector current, respectively.

Figure 1. Cyclic voltammetry generation-collection experiments in 5.0 m**M** $Ru(NH_3)_6Cl_3$ in 0.1 **M** aqueous KCl. The 2.74 μm wide generator was swept between +0.3 and -0.6 V vs. SCE while the potential of the collector electrode(s) was held at +0.1 V vs. SCE. Cathodic ($Ru(NH_3)_6^{3+}$ reduction) generator currents and anodic ($Ru(NH_3)_6^{2+}$ oxidation) collector currents, i_a and i_c, are indicated. Curve 1 presents results for a single generator electrode (no collection). Curves 2 and 3 present results for a single generator (lower curve) and a single collector electrode (upper curve) separated by 1.37 μm. Curves 4 and 5 represent results for a single generator (lower curve) and 6 adjacent collector electrodes (upper curve). The various microelectrodes are numbered as indicated in Scheme I.

Figure 2. Cyclic voltammetry for a 10 μm diameter disk platinum microelectrode in pH 7, 0.1 **M** aqueous KCl solution containing 5.0 m**M** of (1) $Ru(NH_3)_6^{2+}$; (2) $Fe(CN)_6^{4-}$; and (3) $Ru(NH_3)_6^{3+}$. The inset shows the concentration dependence of the limiting microdisk current.

Figure 3. Microelectrode transit time measurements for $Ru(NH_3)_6^{2+}$ created at a 1.3 μm wide, 6 μm long generator

microelectrode, as monitored by oxidation at an adjacent, parallel collector microelectrode separated by a gap of 0.8 μm from the generator. Experiments were conducted in 10 m**M** $Ru(NH_3)_6Cl_3$ and 0.1 **M** aqueous KCl. The generator electrode was pulsed from 0.0 to -0.40 V vs. SCE for durations ranging from 2 μs to 2 ms, while the collector electrode is maintained at 0.0 V vs. SCE. The number of redox species, indicated in the figure inset, is measured by integration of the collector current.

Figure 4. Microelectrode transit time measurements for $Ru(NH_3)_6^{2+}$ as a function of distance squared between generator and collector. Experiments were conducted in 2.5 m**M** $Ru(NH_3)_6(ClO_4)_3$; 0.1 **M** aqueous $NaClO_4$ solution at 20°C. The peak pulse times are shown for the movement of $Ru(NH_3)_6^{2+}$ following a 5 ms generation pulse. Specified distances are determined from the center of the 2.74 μm wide generator electrode to the nearest edge of the indicated collector electrode. The solid line in the figure inset is calculated using equation (3) and $D = 7.8 \times 10^{-6}$ cm^2/s.

Figure 5. The time variation of collector current following pulsed generation of $Ru(NH_3)_6^{2+}$ in solutions of varying diffusivity. Experiments were conducted in 2.5 m**M** $Ru(NH_3)_6(ClO_4)_3$ and 0.1 **M** aqueous $NaClO_4$ with varying concentrations of sucrose added using a 5 ms generation

pulse. In the inset the solid line was calculated using equation (3).

Figure 6. Time dependence of collector current following stepped generation of $Ru(NH_3)_6^{2+}$ as a function of distance between generator and collector. Experiments were conducted in 2.5 m**M** $Ru(NH_3)_6(ClO_4)_3$ and 0.1 **M** aqueous $NaClO_4$. The generator electrode was stepped from 0.0 to -0.4 V vs. SCE, while the collector electrode is maintained at 0.0 V vs. SCE. Electrode width and separation is shown in Scheme I; the indicated distances are determined from the center of the generator electrode to the nearest edge of the collector electrode.

Figure 7. Plots of $t_{1/3}$ and $t_{2/3}$ vs. $(\text{distance})^2$ from curves as shown in Figure 6. The solid lines are for $t_{1/3}$ and $t_{2/3}$ using equations (4) and (5), respectively.

Figure 8. Variation of $t_{1/3}$ and $t_{2/3}$ values (from curves like those in Figure 6) with changes in solution viscosity. Experiments were conducted in 2.5 m**M** $Ru(NH_3)_6(ClO_4)_3$; 0.1 **M** aqueous $NaClO_4$ electrolyte containing various concentrations of sucrose at 20°C. The generator electrode was stepped from 0.0 to -0.4 V vs. SCE, while the collector electrode was maintained at 0.0 V vs. SCE. Solutions contained 0%, 10%, 15%, 20%, 26%, 34%, 40%, or 48% by weight of sucrose,

with respective viscosities ranging from η = 1.00 to 12.5 cP.

Figure 9. Geometry used for the two-dimensional random walk simulation of generation-collection microelectrode experiments. A cross sectional plane of the parallel microelectrodes is depicted in which a pulse or a continuous generation of concentration units are introduced into the model at the indicated generator site. Each of these redox units, characterized by diffusion coefficient, D, will randomly move a distance, ΔX (set equal to the experimental inter-electrode gap of 1.37 μm), during each iterative time cycle of duration $(\Delta X)^2/4D$. Redox units arriving at any activated collector site are counted and removed from solution to indicate collection, Scheme I, as a function of time.

Figure 10. Concentration profiles at times 10, 100, and 500 ms after the release of 10^5 species from the generator electrode in a random walk simulation as described in Figure 9. The simulated diffusion coefficient is 7.8×10^{-6} cm^2/s to simulate results experimentally obtained for $Ru(NH_3)_6^{2+}$ in aqueous solution. The percentages shown give the fraction of generated species collected at each time. (Left) The generator electrode releases 10^5 redox units and no collector electrodes collect the released species. (Center) The generator releases 10^5 redox units with a

single asymmetrically disposed collector, three electrodes away. (Right) The generator releases 10^5 redox units with two symmetrically disposed collectors, three electrodes away from the generator. The shading represents the concentration of released species with the darkest shading corresponding to the highest concentration.

Figure 11. A comparison of experimental and simulated steady-state collection efficiencies, Φ_{SS}, at various separations of generator and collector microelectrodes. Collection efficiencies in 5 m**M** $Ru(NH_3)_6Cl_3$ in 0.1 **M** aqueous KCl are determined from steady-state currents as indicated in Figure 1. Diamond, square and open triangles refer respectively to experimental, theoretical (this work) and theoretical (from reference 12) collection efficiencies for an asymmetric individual collector electrode located on a single side of the generator electrode. '+', 'X' and solid triangles refer similarly to experimental, theoretical (this work) and theoretical (from reference 12) collection efficiencies for a pair of collector electrodes situated symmetrically about a central generator. Separations used are the measured center to center distance for comparison with the theory in reference 12.

Figure 12. A comparison of experimental and simulated steady-state collection efficiencies, Φ_{SS}, for various total widths of collector microelectrodes. Collection

efficiencies in 5 m**M** $Ru(NH_3)_6Cl_3$; 0.1 **M** aqueous KCl are determined from steady-state currents as in Figure 1. Diamond and squares refer respectively to experimental and theoretical (this work) collection efficiencies utilizing from n = 1 to 7 nearest collector electrodes located on a single side of the generator electrode. '+', 'X' and solid triangles refer respectively to experimental, theoretical (this work) and theoretical (from reference 12) collection efficiencies for 2, 4, 6 or 7 nearest collector electrodes situated about a central generator. Total collector width is given by 2.74 x n μm.

Figure 13. Simulated and experimental dynamic transit time measurements for movement of $Ru(NH_3)_6^{2+}$, with a diffusion coefficient of 7.8×10^{-6} cm^2/s, between adjacent microelectrodes 2.74 μm wide and separated by a 1.37 μm. The simulation was performed for 10^5 redox units.

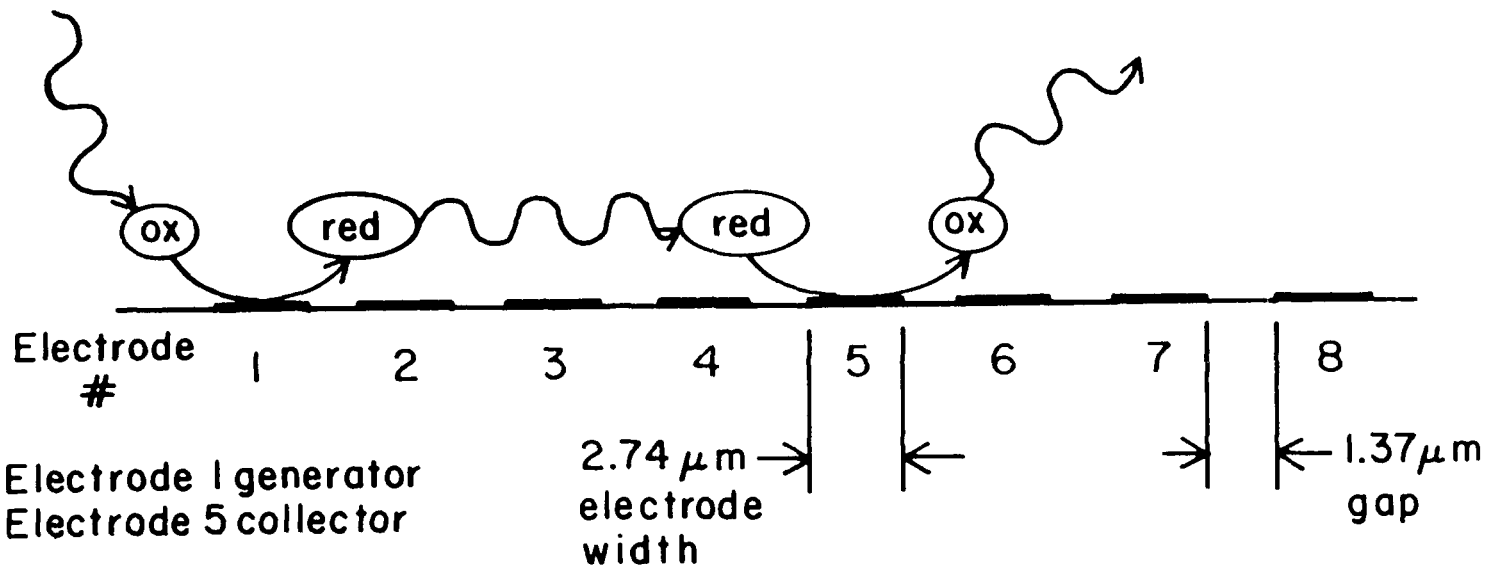
ox
red
red
ox
Electrode #
1
2
3
4
5
6
7
8
Electrode 1 generator
Electrode 5 collector
2.74 μm
electrode
width
1.37 μm
gap

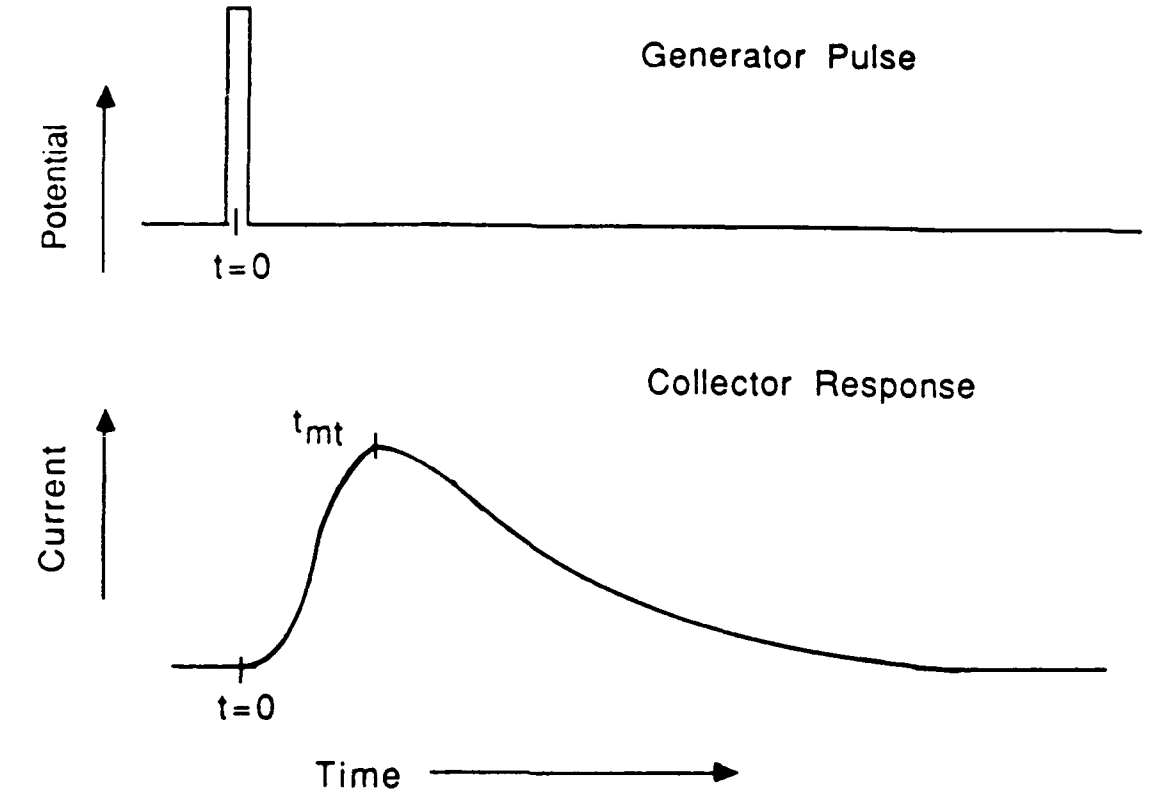
Generator Pulse
Potential
t=0
Collector Response
Current
t_{mt}
t=0
Time

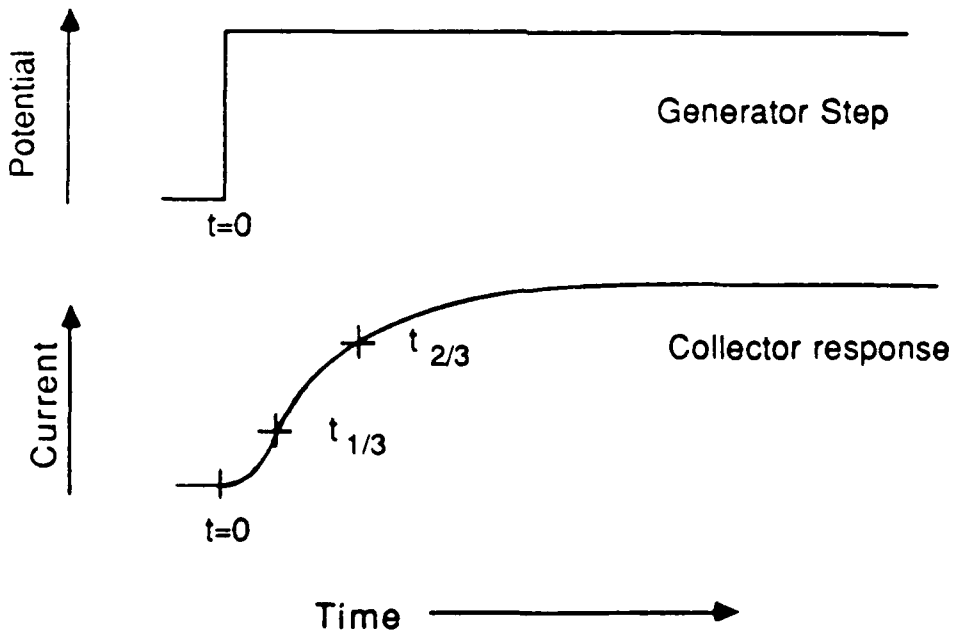
Potential
Generator Step
t=0
Current
$t_{2/3}$
Collector response
$t_{1/3}$
t=0
Time

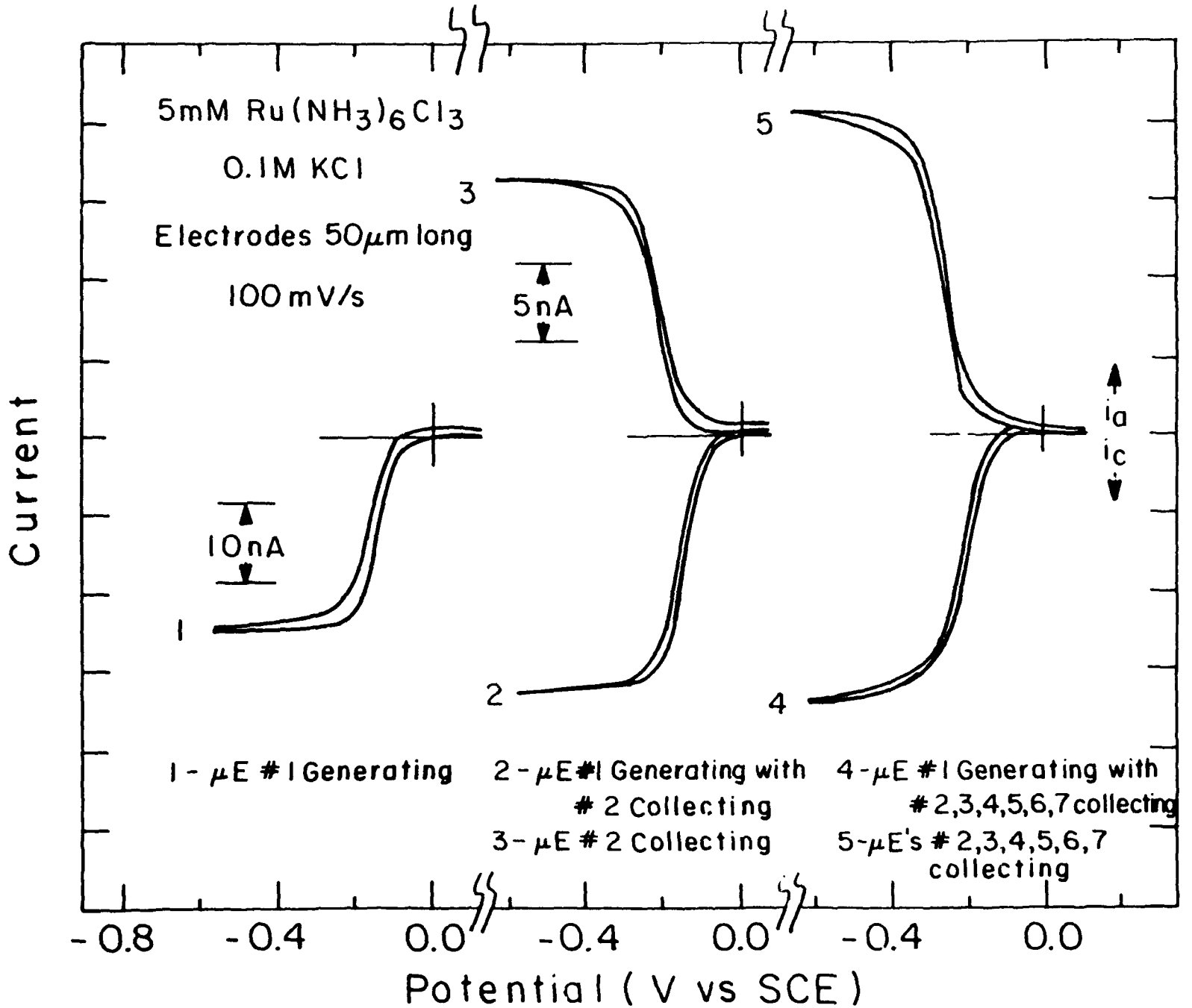
5mM Ru(NH3)6Cl3
0.1M KCl
Electrodes 50μm long
100 mV/s
10nA
5nA
ia
ic
1
2
3
4
5
Current
1 - μE #1 Generating
2 - μE #1 Generating with #2 Collecting
3 - μE #2 Collecting
4 - μE #1 Generating with #2,3,4,5,6,7 collecting
5 - μE's #2,3,4,5,6,7 collecting
-0.8
-0.4
0.0
-0.4
0.0
-0.4
0.0
Potential (V vs SCE)

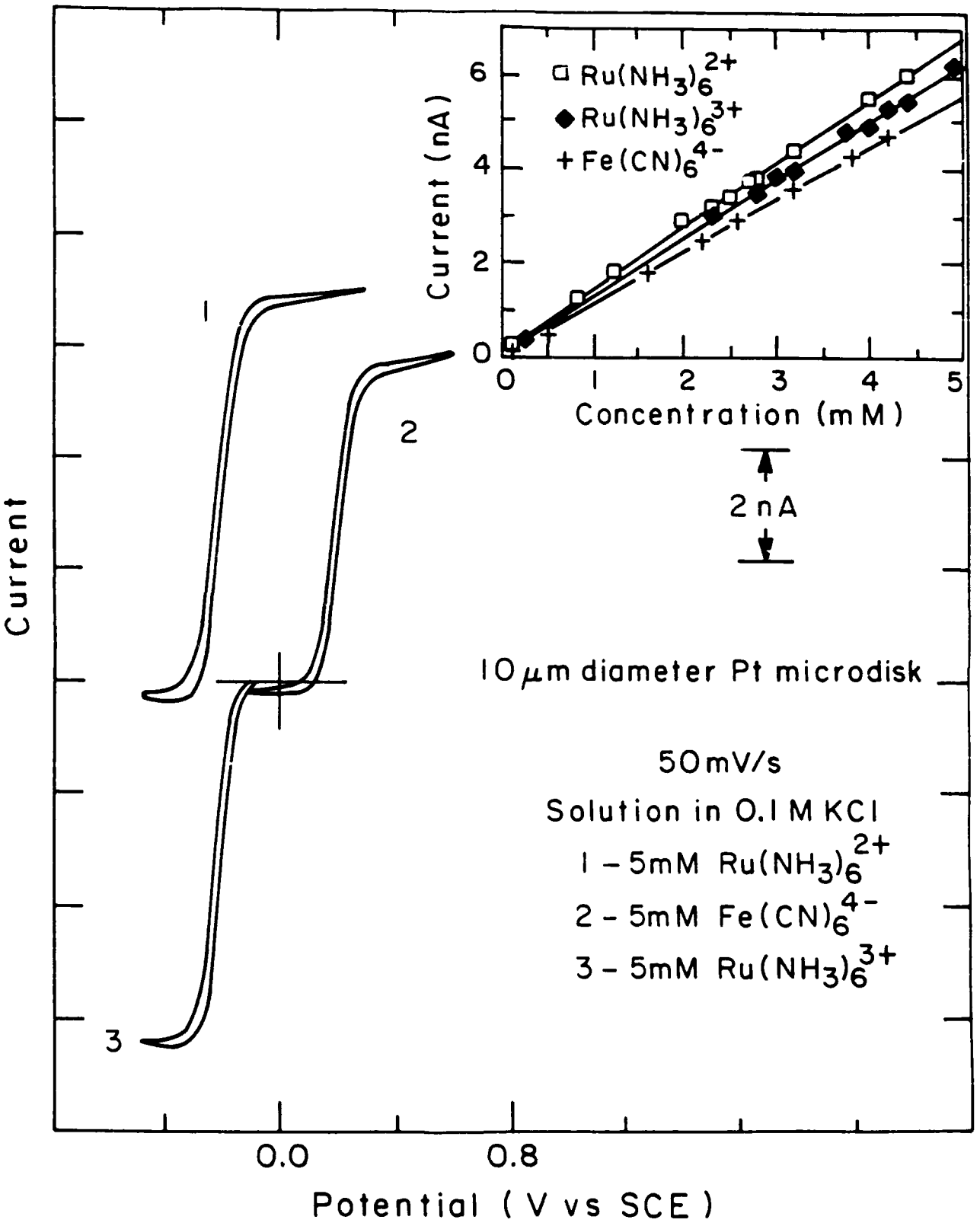
Current (nA)
6
4
2
0
□ Ru(NH3)6 2+
◆ Ru(NH3)6 3+
+ Fe(CN)6 4-
0 1 2 3 4 5
Concentration (mM)
2 nA
Current
1
2
3
10 μm diameter Pt microdisk
50 mV/s
Solution in 0.1 M KCl
1 - 5mM Ru(NH3)6 2+
2 - 5mM Fe(CN)6 4-
3 - 5mM Ru(NH3)6 3+
0.0
0.8
Potential (V vs SCE)

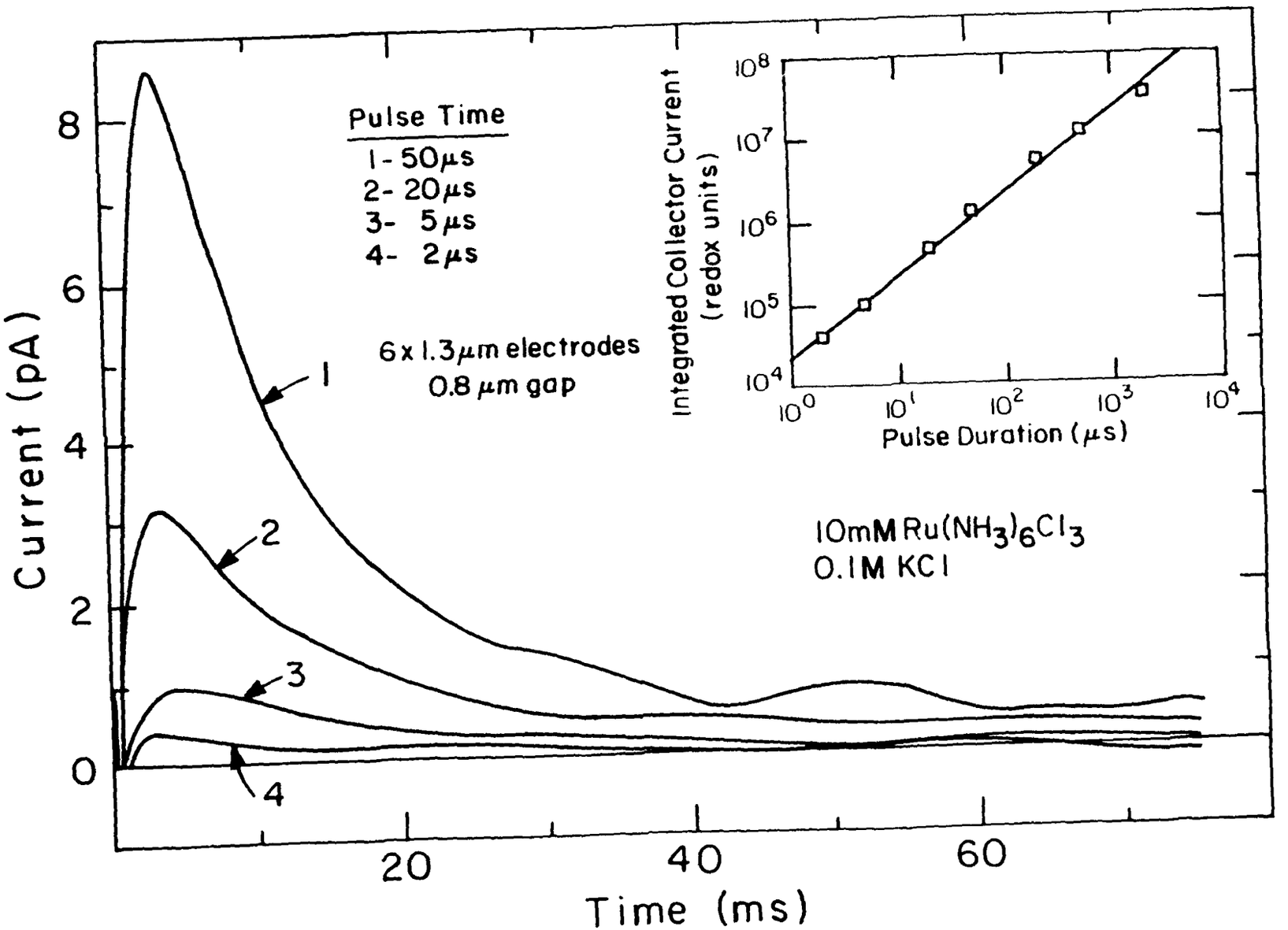
Pulse Time
1- 50μs
2- 20μs
3- 5μs
4- 2μs
6 x 1.3μm electrodes
0.8 μm gap
10mM Ru(NH3)6Cl3
0.1M KCl
Current (pA)
Time (ms)
Integrated Collector Current (redox units)
Pulse Duration (μs)

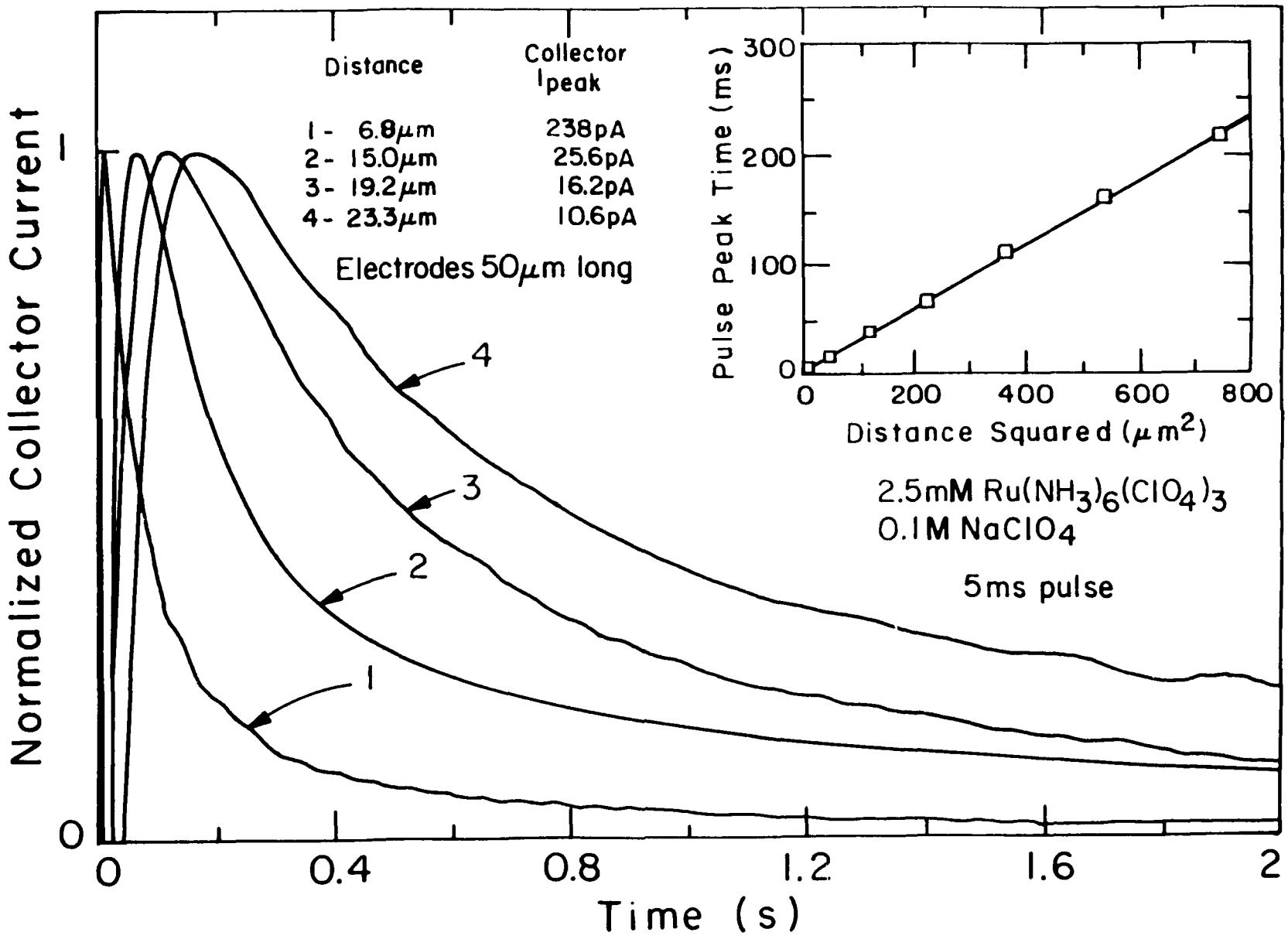
Distance
Collector Ipeak
1 - 6.8μm 238pA
2 - 15.0μm 25.6pA
3 - 19.2μm 16.2pA
4 - 23.3μm 10.6pA
Electrodes 50μm long
Normalized Collector Current
0
0
0.4
0.8
1.2
1.6
2
Time (s)
1
2
3
4
Pulse Peak Time (ms)
300
200
100
0
0
200
400
600
800
Distance Squared (μm²)
2.5mM Ru(NH3)6(ClO4)3
0.1M NaClO4
5ms pulse

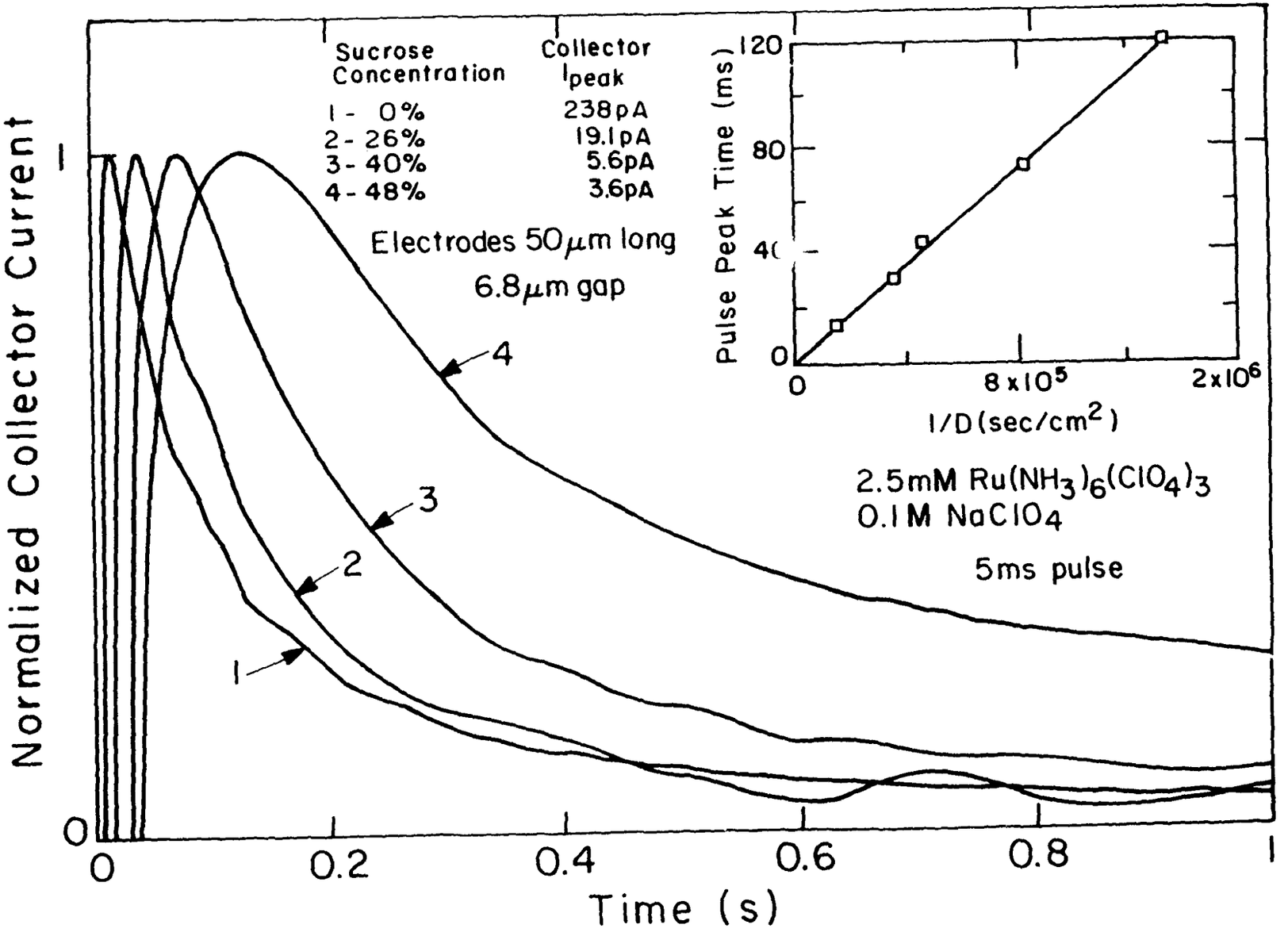
Sucrose Concentration
Collector I_{peak}
1 - 0% 238pA
2 - 26% 19.1pA
3 - 40% 5.6pA
4 - 48% 3.6pA
Electrodes 50μm long
6.8μm gap
2.5mM $Ru(NH_3)_6(ClO_4)_3$
0.1M $NaClO_4$
5ms pulse
Normalized Collector Current
Time (s)
0
0.2
0.4
0.6
0.8
1
Pulse Peak Time (ms)
120
80
40
0
8×10^5
2×10^6
1/D (sec/cm^2)

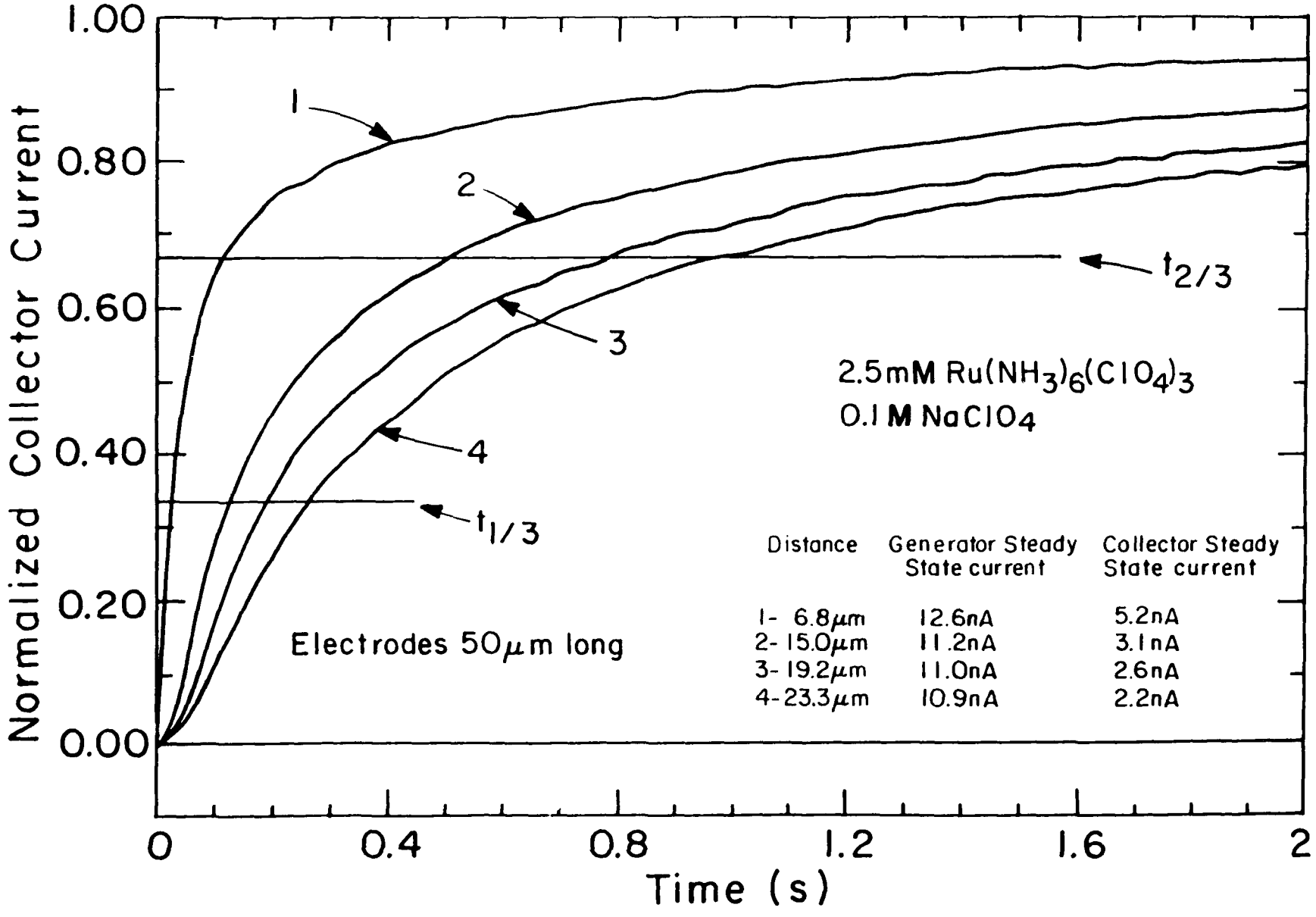
1.00
0.80
0.60
0.40
0.20
0.00
Normalized Collector Current
0
0.4
0.8
1.2
1.6
2
Time (s)
1
2
3
4
$t_{2/3}$
$t_{1/3}$
2.5mM $Ru(NH_3)_6(ClO_4)_3$
0.1 M $NaClO_4$
Electrodes 50μm long
Distance
Generator Steady State current
Collector Steady State current
1- 6.8μm 12.6nA 5.2nA
2- 15.0μm 11.2nA 3.1nA
3- 19.2μm 11.0nA 2.6nA
4- 23.3μm 10.9nA 2.2nA

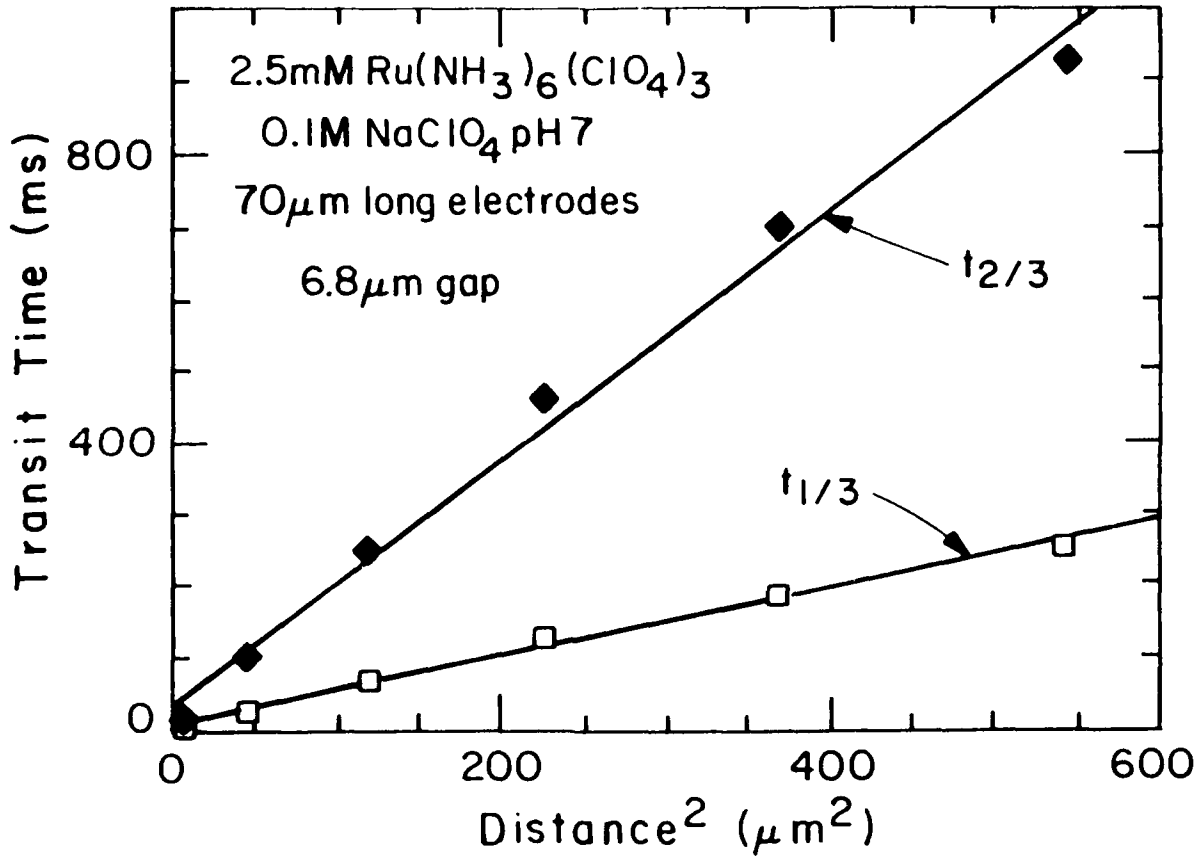
2.5mM Ru(NH3)6(ClO4)3
0.1M NaClO4 pH 7
70μm long electrodes
6.8μm gap
t2/3
t1/3
Transit Time (ms)
800
400
0
0
200
400
600
Distance2 (μm2)

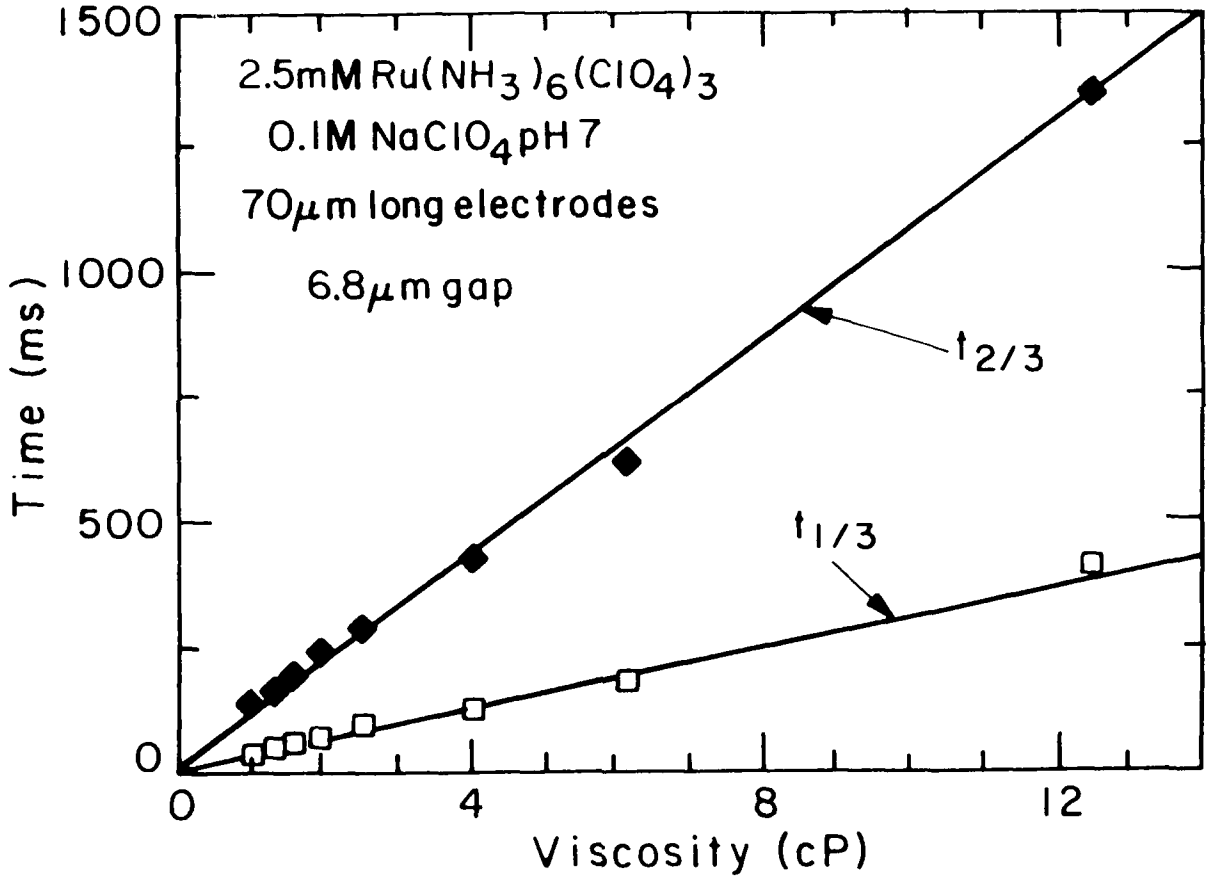
1500
1000
500
0
Time (ms)
2.5mM Ru(NH3)6(ClO4)3
0.1M NaClO4 pH 7
70μm long electrodes
6.8μm gap
t2/3
t1/3
0
4
8
12
Viscosity (cP)